Exchange-correlation effects on the hole miniband structure and confinement potential in zinc-blende $Al_xGa_{1-x}N$/GaN superlattices

2001 J. Phys.: Condens. Matter 13 3381

(http://iopscience.iop.org/0953-8984/13/14/311)

INSTITUTE OF PHYSICS PUBLISHING JOURNAL OF PHYSICS: CONDENSED MATTER

J. Phys.: Condens. Matter **13** (2001) 3381–3387 www.iop.org/Journals/cm PII: S0953-8984(01)21390-3

Exchange–correlation effects on the hole miniband structure and confinement potential in zinc-blende $Al_xGa_{1-x}N/GaN$ superlattices

S C P Rodrigues, G M Sipahi, L M R Scolfaro and J R Leite

Instituto de Física da Universidade de São Paulo, CP 66318, 05315-970 São Paulo, SP, Brazil

E-mail: srodrigu@macbeth.if.usp.br (S C P Rodrigues)

Received 25 January 2001

Abstract

We present valence band-structure calculations for undoped and p-doped cubic $Al_xGa_{1-x}N/GaN$ superlattices (SLs), in which the coupling between the heavy-hole, light-hole, and spin–orbit-split-hole bands and strain effects due to lattice mismatch are taken into account. The calculations are performed within a self-consistent approach to the $\boldsymbol{k}\cdot\boldsymbol{p}$ theory by means of a full six-band Luttinger–Kohn Hamiltonian. Exchange–correlation effects within the two-dimensional hole gas are included in the calculations in the local density approximation. Results for hole minibands and potential profiles are shown as functions of the SL period. It is shown that exchange and correlation play an important role in the correct description of the systems.

1. Introduction

The III–V nitride semiconductors GaN, AlN, and AlGaN exhibit interesting physical properties such as high thermal conductivity, large band-gap energies, and both conduction and valence band offsets for carrier confinement. They are attractive for optoelectronic device applications in the blue–ultraviolet spectral region, as well as at high power and high temperature [1, 2]. Although most of the progress achieved so far is based on the hexagonal (wurtzite) phase of the materials, the cubic (c) metastable phase is seen as an advantageous and promising alternative for similar applications [3, 4]. For devices, the production of highly conductive p-type GaN and AlGaN layers is of crucial importance. However, controlled doping and its efficiency, especially in AlGaN alloys, have been limited by the level of the acceptor (usually Mg, C, or Be) being deep: it lies at around 0.2 eV [5, 6]. Recently, several attempts have been made to enhance the acceptor doping efficiency by using multiple quantum wells and superlattices (SLs) made up of alternate layers of AlGaN and GaN. It has been demonstrated that p-doping of $Al_xGa_{1-x}N/GaN$ SLs increases the free-hole concentration as compared to that of bulk p-type GaN [7, 8]. It has been proposed that piezoelectric (PZ) field effects cause free-carrier enhancement in $Al_xGa_{1-x}N/GaN$ SLs [9–12]. Contrary to the case for wurtzite structures, in p-doped c-AlGaN/GaN the free-hole concentration can be higher, even in the

0953-8984/01/143381+07$30.00

absence of PZ fields. Despite the potentiality recently suggested for cubic-structure-derived AlGaN heterostructures, very little is known about their hole sub-band structure and potential profiles, particularly for p-doped systems [13].

In this work we study the valence band structure and the two-dimensional hole gas (2DHG) in p-doped c-$Al_xGa_{1-x}N$/GaN SLs by carrying out self-consistent band-structure calculations within the $\boldsymbol{k}\cdot\boldsymbol{p}$ model in a plane-wave representation. The 6×6 Luttinger–Kohn (LK) effective-mass and Poisson equations are solved self-consistently, including many-body effects such as exchange and correlation within the local density approximation. The role played by strain effects on the hole sub-bands and minibands is analysed. We discuss particularly the effects of exchange and correlation on the band structure and potential profiles.

2. The method applied to heterostructures

We adopt an approach using a super-cell model that comprises the barrier (thickness d_1) and the well (thickness d_2) regions of the SL. The method is an extension of a previous version developed to study p–delta-doping layers in GaAs and Si [14–16]. We assume an infinite SL of square wells along the [001] direction. Figure 1 shows schematically one superlattice period. The multiband effective-mass equation (EME) is represented with respect to plane waves with wavevectors $K = (2\pi/d)l$ (l an integer and d the SL period) equal to reciprocal SL vectors. The rows and columns of the 6×6 LK Hamiltonian relate to the Bloch-type eigenfunctions $|jm_j\boldsymbol{k}\rangle$ of the Γ_8 heavy- and light-hole bands, and the Γ_7 spin–orbit-split-hole band; $\boldsymbol{k}$ denotes a vector of the first SL Brillouin zone (BZ) shown schematically in figure 2. Expanding the EME with respect to plane waves $(z|K)$ means representing this equation in terms of the Bloch functions $(\boldsymbol{x}|jm_j\boldsymbol{k}+K\boldsymbol{e}_z)$. For a Bloch-type eigenfunction $(z|E\boldsymbol{k})$ of the SL of energy E and

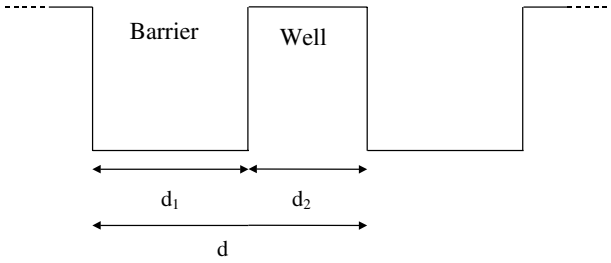

Figure 1. A schematic representation of a superlattice emphasizing one period d, with barrier thickness d_1 and well thickness d_2.

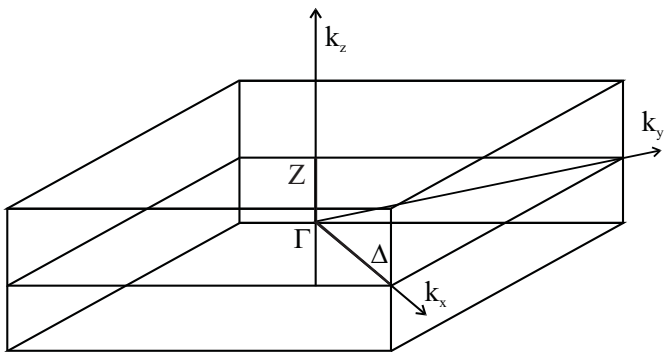

Figure 2. The first Brillouin zone of the superlattice. Γ–Z represents a symmetry line along the growth direction and Γ–Δ represents a symmetry line along the direction k_x, perpendicular to the SL axis.

wavevector $\boldsymbol{k}$, the EME takes the form

$$\sum_{j'm'_jK'} (jm_j\boldsymbol{k}K|T + H_S + V_{HET} + V_C + V_{xc}|j'm'_j\boldsymbol{k}K')(j'm'_j\boldsymbol{k}K'|E\boldsymbol{k}) = E(\boldsymbol{k})(j'm'_j\boldsymbol{k}K') \quad (1)$$

where T is the unperturbed kinetic energy term, generalized for a heterostructure [17], H_S is the strain energy term originating from the lattice mismatch, V_{HET} is the square potential due to the difference between the energy gaps, V_{xc} is the exchange–correlation potential, and V_C is the Coulomb potential given by the sum of the Hartree potential and the ionized acceptor potential. The self-consistent potentials and charge densities are obtained by solving the multiband EME (equation (1)) and the Poisson equation given by

$$(jm_j\boldsymbol{k}K|V_C|j'm'_j\boldsymbol{k}K') = \frac{4\pi e^2}{\kappa}\frac{1}{|K-K'|^2}(K|p - N_A|K')\delta_{jj'}\,\delta_{m_jm'_j} \quad (2)$$

where κ is the dielectric constant ($\kappa = 9.5$ for GaN [2]), and where N_A is the acceptor doping concentration and p is the hole charge distribution, both expressed in the plane-wave representation. Details of the theoretical model can be found elsewhere [14].

The Luttinger parameters and other parameters used in the calculations are taken for each epitaxial layer of the SL. A biaxial compressive strain is considered which is decomposed into two parts: a hydrostatic strain and a uniaxial strain. The former shifts the gap energy; thus it does not influence the confined hole levels. The latter changes the valence band potential depth and may be calculated assuming that the strain, $\epsilon(z)$, is zero in the barrier, and is given inside the well by the Fourier coefficients of [13, 17]:

$$\epsilon(z) = -(2/3)D_u\epsilon_\parallel(1 + 2C_{12}/C_{11}) \quad (3)$$

where $-(2/3)D_u$ is the shear deformation potential, C_{11} and C_{12} are the elastic constants, and $\epsilon_\parallel = (a_b - a_w)/a_w$ is the lattice mismatch, with a_b and a_w being the lattice parameters of the unstrained barrier and the well, respectively. We can then express the strain term of the Hamiltonian, H_S, as follows:

$$(jm_j\boldsymbol{k}K|H_S|j'm'_j\boldsymbol{k}K') = (K|\epsilon(z)|K')M_{jm_j}^{j'm'_j} \quad (4)$$

where $M_{jm_j}^{j'm'_j}$ is defined as

$$M_{jm_j}^{j'm'_j} = \begin{pmatrix} -1 & 0 & 0 & 0 & 0 & 0 \\ 0 & 1 & 0 & 0 & -i\sqrt{2} & 0 \\ 0 & 0 & 1 & 0 & 0 & -i\sqrt{2} \\ 0 & 0 & 0 & -1 & 0 & 0 \\ 0 & i\sqrt{2} & 0 & 0 & 0 & 0 \\ 0 & 0 & i\sqrt{2} & 0 & 0 & 0 \end{pmatrix}. \quad (5)$$

The square potential (V_{HET}) is diagonal with respect to jm_j, $j'm'_j$, and is defined by

$$(jm_j\boldsymbol{k}K|V_{HET}|j'm'_j\boldsymbol{k}K') = (K|V_{HET}|K')\delta_{jj'}\delta_{m_jm'_j} \quad (6)$$

where $(K|V_{HET}|K')$ are the Fourier coefficients of V_{HET}.

The exchange–correlation effects were taken into account in the local density approximation (LDA), by adopting a parametrized expression for an inhomogeneous hole gas of heavy, light, and spin–orbit-split-off holes. The expressions for the exchange–correlation term may be found in our previous works [15, 16]; thus no further details will be provided here.

In table 1 we show the bulk parameters used in the calculations, obtained from *ab initio* full-potential linear augmented-plane-wave (FLAPW) band-structure calculations performed

Table 1. Bulk parameters as obtained from *ab initio* FLAPW calculations performed by us (reference [18]) and extracted from the literature. The effective masses along [001] are in units of the free-electron mass.

	AlN	GaN
γ_1	1.57	2.83
γ_2	0.36	0.85
γ_3	0.60	1.14
Δ (meV)	19	14
a (Å)	4.40	4.55
m^*_{HH}	1.29	0.85
m^*_{LH}	0.41	0.22
m^*_{SO}	0.60	0.34
E^{Γ}_{g}(meV) [2]	6.0	3.2
(2/3)D_{u} (eV)	1.5 [19]	1.6 [20]
C_{11} (GPa) [21]	304	293
C_{12} (GPa) [21]	160	159

by us [18] or extracted from the literature. For the alloys, all of the parameters were interpolated linearly. We adopted 40% for the valence band offset and we assumed in the calculations that the acceptor level is located at about 0.2 eV above the top of the valence band in bulk GaN and AlGaN [5].

3. Results and discussion

First we will discuss the results for undoped AlGaN/GaN SLs. Figure 3 shows the miniband dispersions along the growth direction Γ–Z for undoped and *unstrained* $Al_{0.1}Ga_{0.9}N$/GaN SLs as a function of the well width d_2 (barrier width $d_1 = d_2$). The hole levels are labelled according to their main character at Γ. The notation SOi–LHi (LHi–SOi) means that the mixing character of band i is dominated by the SO (LH). Since the spin–orbit splitting in the nitrides is very small ($\Delta \approx 14$ meV for GaN) [2], the LH and SO levels are already coupled at the Γ point. In figure 3, the SL period is varied from $d_1 = d_2 = 30$ to 60 Å. When the SL period increases, the interaction between the wells decreases, so the miniband dispersion becomes smaller and the levels are deeper in the well, as expected. Only for very short periods ($\leqslant$40 Å) do the minibands appear significantly broader, mainly for SO- and LH-derived bands. This is due to the high values of the effective masses in the nitrides—especially the heavy-hole mass (see table 1).

Similar results are depicted in figure 4, now for *strained* $Al_xGa_{1-x}N$/GaN SLs (with $x = 0.3$). In the systems of figure 3 we assumed that the strain in the barrier and the well were compensated, due to the small value of x. On the other hand, in figure 4 the layers are compressively strained inside the well. However, it is worth pointing out that the critical thickness in these nitrides is still under discussion in the literature [22, 23]. In figure 4 the hole levels are deeper in energy due to the higher value of the barrier height, which places more hole bands as confined within the well. Minibands occur only for higher-lying levels, and for $d_1 = d_2 \leqslant 45$ Å. The compressive strain affects the potential felt by the holes in the following way: the heavy- and split-off-hole potentials become deeper while the light-hole potential becomes shallower. As a consequence, the lower levels are HH and SO–LH ones. Here, once again the high effective-mass values also contribute to this behaviour.

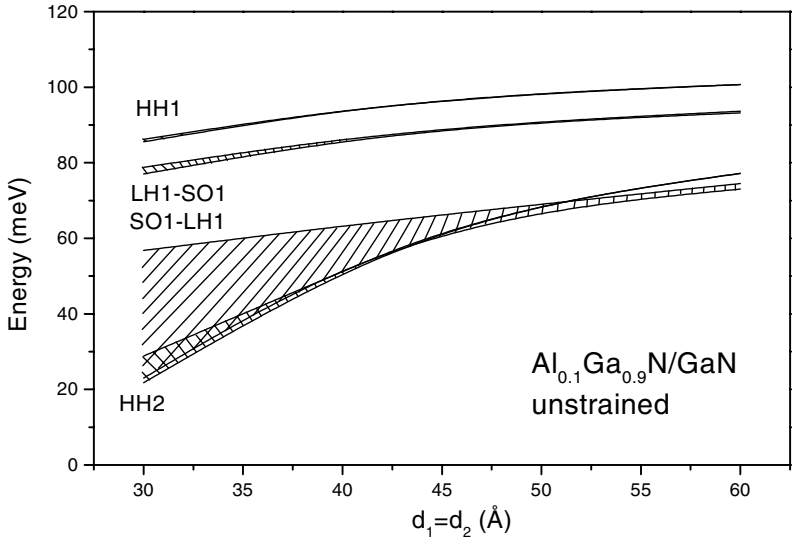

Figure 3. Confined hole energies as a function of the well width d_2 (barrier width $d_1 = d_2$) for undoped and *unstrained* $Al_{0.1}Ga_{0.9}N$/GaN SLs. The well depth equals 109.6 meV. The shaded areas correspond to the miniband dispersions along Γ–Z. The energy zero was taken to be at the top of the AlGaN barrier.

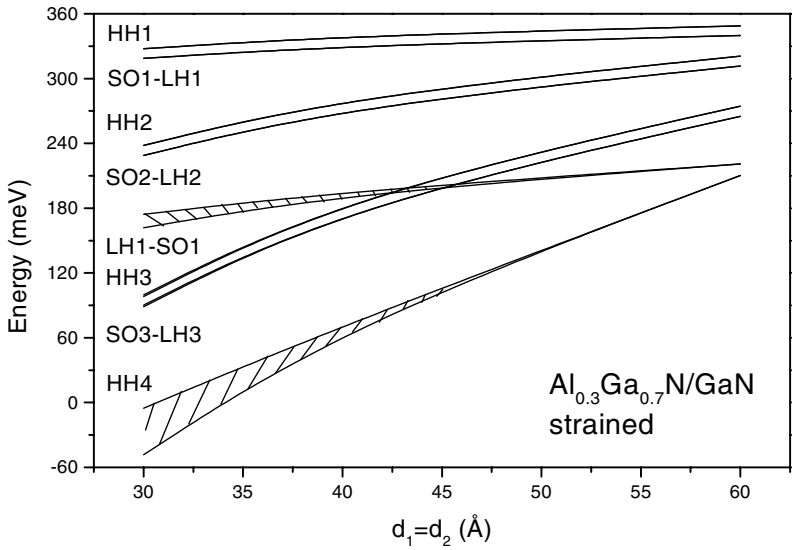

Figure 4. Confined hole energies as a function of the well width d_2 (barrier width $d_1 = d_2$) for *strained* $Al_{0.3}Ga_{0.7}N$/GaN SLs. The strain energy is 33 meV. The well depth equals 328.8 meV. The shaded areas and energy zero are as in figure 3.

We will discuss now the effects of p-doping in AlGaN/GaN SLs. In figure 5 we show the self-consistent hole sub-bands and potential profiles obtained for a fully p-doped-barrier $Al_xGa_{1-x}N$/GaN SL ($x = 0.3$), with $N_A = 1 \times 10^{18}$ cm^{-3}, well width (d_2) of 30 Å, and barrier width (d_1) of 60 Å. An *unstrained* SL was assumed. The hole sub-band levels (left-hand panel in figure 5) for an equivalent situation but neglecting exchange–correlation effects

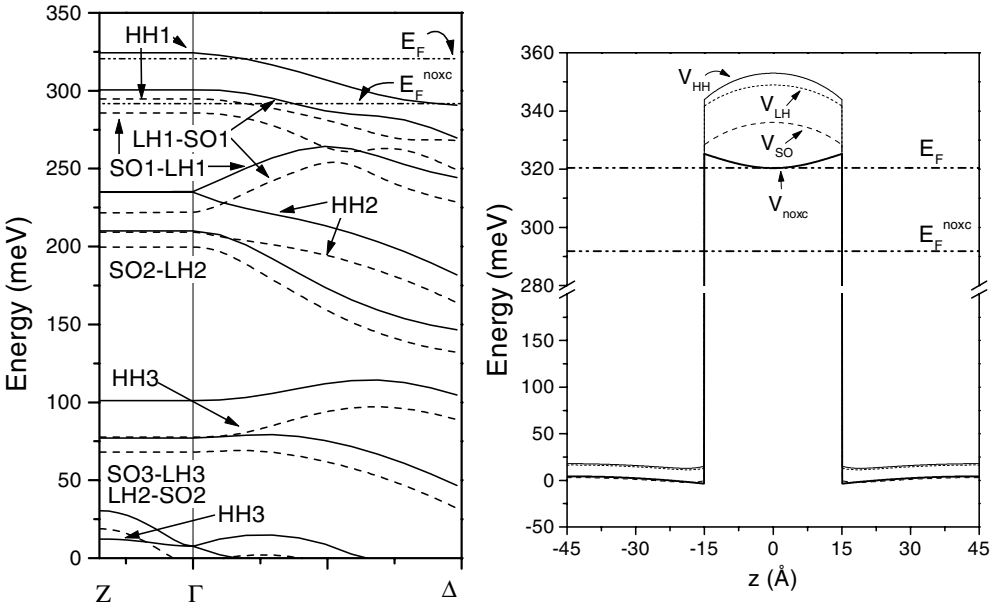

Figure 5. The fully p-doped-barrier $Al_{0.3}Ga_{0.7}N$/GaN SL (*unstrained*), with $d_1 = 60$ Å, $d_2 = 30$ Å, and $N_A = 1 \times 10^{18}$ cm^{-3} (the equivalent two-dimensional hole concentration is $N_{2D} = 6 \times 10^{11}$ cm^{-2}). Left-hand panel: hole sub-bands along (solid lines) the SL symmetry lines Γ–Z (growth axis) and Δ (perpendicular to the growth axis). Hole levels for which exchange–correlation effects have been neglected (dashed lines) are also shown for comparison. Right-hand panel: V_{HH} (solid line), V_{LH} (dotted line), and V_{SO} (dashed line) are the heavy-, light- and split-off-hole potentials, respectively. E_F (dash–dotted line) indicates the Fermi level. V_{noxc} (thick solid line) and E_F^{noxc} (dash–dotted line) are the heavy-hole potential and the Fermi level, respectively, without exchange–correlation effects. Note that V_{SO} is shifted by the spin–orbit splitting, 14 meV, relative to V_{HH}. The energy zero was placed at the top of the Coulomb potential at the AlGaN barrier.

are also shown (dashed lines) for comparison. It is clearly seen that for this short-period SL no miniband dispersion of the low-lying levels occurs (a small dispersion may be observed only for very high hole bands which appear close to the top of the AlGaN barrier). It is interesting to note that the exchange–correlation effects drastically modify the behaviour of the valence band structure, as well as the potential bending (right-hand panel in figure 5) which has its shape completely changed. The contributions for the total potential due to the Coulomb potential V_{noxc} and due to the exchange–correlation potential are very important, since their sum will determine the shape of the bending of the total potential inside the well. This is a consequence of the charge-density localization, which in these short-period SLs is mostly concentrated at the centre of the well. Once the exchange–correlation potential depends on the local charge density, it dominates over the Coulomb potential, thus determining the self-consistent total potential. It is found that only one heavy-hole level, HH1, is occupied. This is also due to the high value of the heavy-hole effective mass for the nitrides. In spite of the occupation of only the first heavy-hole state, the light- and split-off-hole bands cannot be neglected. Moreover, while the splitting between the HH1 and the LH1–SO1 levels is of ≈10 meV in the calculation which neglects exchange–correlation effects, it reaches a value of ≈25 meV when these effects are taken into account. The Fermi level also changes by approximately 30 meV. These findings will certainly have important implications for optical measurements, such as in luminescence or absorption experiments.

In summary, our investigations show that the effects of strain and of the inclusion of the spin–orbit interaction play an important role in the description of the valence band structure in undoped and p-doped AlGaN/GaN SLs. Hole minibands with significant dispersion occur only for small well widths ($\leqslant$40 Å). The exchange–correlation effects within the 2DHG are crucial for explaining the different behaviour observed in the potential bending. As in other systems involving confined hole gases [14,15], the present results show that also in modulation-p-doped AlGaN/GaN heterostructures, the many-body effects, such as exchange and correlation, must be taken into account for a realistic description of the hole bands and potentials in these systems.

Acknowledgments

We would like to thank the Brazilian funding agencies FAPESP and CNPq for partial support.

References

[1] Orton J W and Foxon C T 1998 *Rep. Prog. Phys.* **61** 1
[2] Edgar J H (ed) 1994 *Properties of Group-III Nitrides* (London: INSPEC)
[3] As D J, Richter A, Busch J, Lübbers M, Mimkes J and Lischka K 2000 *Appl. Phys. Lett.* **76** 13
[4] Wu J, Yaguchi H, Onabe K and Shiraki Y 1999 *J. Cryst. Growth* **197** 73
[5] Pankove J I and Moustakas T D (ed) 1998 *Gallium Nitride (GaN): I (Semiconductors and Semimetals vol 50)* (San Diego, CA: Academic)
[6] Marques M, Ramos L E, Scolfaro L M R, Teles L K and Leite J R 2001 *Proc. 25th Int. Conf. on Physics of Semiconductors (Osaka, Japan)* at press
[7] Kozodoy P, Hansen M, DenBaars S P and Mishra U K 1999 *Appl. Phys. Lett.* **74** 3681
[8] Saxler A, Mitchel W C, Kung P and Razeghi M 1999 *Appl. Phys. Lett.* **74** 2023
[9] Hsu L and Walukiewicz W 1999 *Appl. Phys. Lett.* **74** 2405
[10] Goepfert I D, Schubert E F, Osinsky A, Norris P E and Faleev N N 2000 *J. Appl. Phys.* **88** 2030
[11] Kumakura K, Makimoto T and Kobayashi N 2000 *Japan. J. Appl. Phys.* **39** 2428
[12] Kumakura K and Kobayashi N 1999 *Japan. J. Appl. Phys.* **38** L1012
[13] Rodrigues S C P, Scolfaro L M R, Leite J R and Sipahi G M 2000 *Proc. Int. Workshop on Nitride Semiconductors (IPAP Conf. Ser. vol 1)* p 74
[14] Sipahi G M, Enderlein R, Scolfaro L M R and Leite J R 1996 *Phys. Rev.* B **53** 9930
[15] Rosa A L, Scolfaro L M R, Enderlein R, Sipahi G M and Leite J R 1998 *Phys. Rev.* B **58** 15 675
[16] Enderlein R, Sipahi G M, Scolfaro L M R and Leite J R 1997 *Phys. Rev. Lett.* **79** 3712
Enderlein R, Sipahi G M, Scolfaro L M R and Leite J R 1998 *Phys. Rev. Lett.* **80** 3160
[17] Rodrigues S C P, Scolfaro L M R, Leite J R and Sipahi G M 2000 *Appl. Phys. Lett.* **76** 1015
[18] Ramos L E, Teles L K, Scolfaro L M R, Castineira J L P, Rosa A L and Leite J R 2001 *Phys. Rev.* B **63** at press
[19] Van de Walle C G and Neugebauer J 1997 *Appl. Phys. Lett.* **70** 2577
[20] Fan W J, Li M F, Chong T C and Xia J B 1996 *J. Appl. Phys.* **80** 3471
[21] Wright A F 1997 *J. Appl. Phys.* **82** 2833
[22] Frey T, As D J, Bartels M, Pawlis A, Lischka K, Tabata A, Fernandez J R L, Silva M T O, Leite J R, Haug C and Brenn R 2001 *J. Appl. Phys.* at press
[23] Parker C A, Roberts J C, Bedair S M, Reed M J, Liu S X and El-Masry N A 1999 *Appl. Phys. Lett.* **75** 2776